Complete wetting of helium on graphite

G. Zimmerli and M. H. W. Chan
Department of Physics, The Pennsylvania State University, University Park, Pennsylvania 16802
(Received 17 March 1988)

Using the vibrating-wire microbalance technique we have found that superfluid ^{4}He, normal fluid ^{4}He, and ^{3}He all wet graphite completely. Incomplete wetting above T_λ was simulated by intentionally introducing a temperature gradient in the apparatus. Data in the thick-film regime are found to be consistent with the Frenkel-Halsey-Hill model of adsorption. The graphite fiber surface has been characterized through volumetric adsorption isotherms, revealing additional surface area not previously accounted for by others using this technique.

I. INTRODUCTION

There are two distinct growth modes that can occur when an adsorbed film condenses from the vapor phase onto a solid surface as the vapor pressure is increased toward the saturated value. The film is said to wet the substrate if its thickness diverges with increasing pressure. If the thickness of the film remains limited to only a few layers at saturated pressure, nonwetting growth is said to occur. Recent models[1] on wetting propose that in the low-temperature limit it is the relative strength of adsorbate-substrate and adsorbate-adsorbate interactions that determines whether a particular physisorption system will exhibit wetting or nonwetting behavior. When adsorbate-substrate interaction dominates, complete wetting is expected. Since the product of the molecular polarizabilities provides a fairly reliable estimate of the van der Waals interaction between two molecules,[2] an adsorbate of sufficiently small polarizability is expected to wet most substrates. However, experimental studies performed to date appear to show nonwetting growth for a number of solid films of very low polarizabilities.[3] The most reasonable explanation is that the strain induced by structural mismatch between successive solid layers eventually becomes too costly in free energy and wetting is suppressed.[4] This consideration leaves liquid helium to be the ideal system to test the complete wetting prediction in the low-temperature limit.

Although there have been numerous studies on the thickness of adsorbed helium films on a variety of substrates dating back to the 1930s, conflicting results are still being reported. A number of early experiments reported the observation that film thickness is limited to 20 layers below T_λ and a few layers above T_λ. In a series of careful ellipsometric measurements on a polished metal surface that is partially submerged in liquid helium, Jackson and co-workers showed that the film thickness above T_λ can be increased from less than 10 layers to 100 layers, close to but less than that found below T_λ, by minimizing thermal inhomogeneity along the surface.[5] Experimental evidence consistent with complete wetting of ^{4}He on quartz and gold below T_λ were also found by Hemming[6] in another ellipsometry study. The most striking confirmation of complete wetting below T_λ is the acoustic resonance experiment of Sabisky and Anderson[7] performed at 1.38 K on cleaved crystal surfaces. Their experimental result was found to be in quantitative agreement with the theory of Dzyaloshinski, Lifshitz, and Pitaevskii (DLP).[8] Whereas the results of a recent quartz microbalance experiment[9] were interpreted to indicate nonwetting of ^{4}He on Au or Ag between 1 K and the liquid-vapor critical point, complete wetting of ^{4}He on gold is found in an even more recent quartz microbalance experiment.[10] Conflicting results are also being reported for ^{4}He on graphite. A volumetric vapor pressure isotherm study[11] was interpreted to indicate that ^{4}He does not wet graphite above and below T_λ. In contrast, a third sound experiment on graphite fibers[12] shows wetting in the superfluid region. In a recent Letter, Taborek and Senator[13] (TS) reported the observation of a wetting transition in ^{4}He on graphite associated with the onset of superfluidity. Using the vibrating-wire microbalance technique they found complete wetting of superfluid ^{4}He films and incomplete wetting of ^{3}He and normal fluid ^{4}He on graphite and platinum fibers. The vibrating wire microbalance technique used by TS is similar to that developed for viscosity and liquid density measurements.[14] Bartosch and Gregory[15] are the first to adopt this technique to study adsorption of O_2 on graphite surface by using a graphite fiber as the vibrating element. The experiment described below also employs the vibrating graphite fiber technique; in contrast to the experiment of TS, we find complete wetting on graphite by ^{3}He and ^{4}He both above and below T_λ. The thickening of the adsorbed film is found to be consistent with theoretical expectation when the vapor pressure is brought close to the saturation value. In addition, we demonstrate experimentally that a slight thermal gradient can produce a false nonwetting result.

II. GRAPHITE FIBER CHARACTERIZATION

The fibers used in this experiment are mesophase pitch-based P-120 graphite fibers.[16] In this classification, the letter P denotes pitch based and 120 is the value of the tensile modulus in units of million pounds per square inch (MPSI). Different types of fibers are typically

characterized through measurements of tensile modulus, density, thermal and electrical conductivity, electron microscopy, and x-ray line broadening studies. These properties yield information regarding the lattice imperfection of the fibers. What is most relevant for the work reported here is the result of a x-ray line-broadening study.[17] In this study, the crystallite sizes in the c and along basal plane direction is found to be more than 200 Å for the P-120-type fibers. Also important is the fact that electron microscopy studies indicate that although the interior structure is such that the basal planes are oriented radially outward from the center, the exposed surface of the fibers is basal plane.[18] Electron microscopy pictures taken by us, shown in Fig. 1, and others reveal the basal planes on the surface show up as long and narrow facets ($\sim 0.1 \times 10$ μm^2) that run parallel to the fiber axis. Because of the ridge-trough structure of these facets, the surface area available for adsorption is likely to be much larger than that expected for perfect cylindrical cross section. Such an enhancement is clearly observed in our volumetric and vibrating fiber isotherm studies.

Volumetric vapor pressure isotherms as shown in Fig. 2 were performed with ^{4}He at 2.16 K and Xe at 113 K on a large bundle (total mass 2.26 g) of P-120 graphite fibers (density $= 2.18$ g/cm^3). The fiber bundle was heated in a quartz tube to approximately 800 °C in flowing N_2 gas before being placed in a sample cell. For these measurements pressure is read with a commercial capacitance gauge. These isotherms, displaying stepwise growth, are qualitatively similar to that obtained with exfoliated graphite substrates.[11,19,20] Two steps were resolved in the Xe isotherm, the rounding observed for the second layer suggest the basal-plane crystallite size on the fiber surface is on the same order (100×100 Å^2), but clearly less than that of exfoliated substrate such as grafoil. The x-ray line-broadening interpretation of the crystallite size may be somewhat optimistic. We believe that the absence of the third layer in the Xe isotherm which is clearly resolved with exfoliated graphite substrates,[19] reflects the smearing effect of the finite size of single-crystal domains. Figure 3 shows the adsorption of Xe (as reflected by the decrease in resonant frequency) as a function of pressure on a single graphite fiber at 107 K obtained with our microbalance apparatus. Four steps in frequency versus pressure are seen near 0 and at 0.42, 0.73, and 0.84 Torr. Other than that at the lowest pressure, these signatures correspond to stepwise formation of adsorbed layers on graphite. As we shall discuss below, the first step is due to adsorption of the first layer and the hydrodynamic drag of the vapor. Figure 3 is obtained with an experimental fiber P130-X, also from Amoco Performance Products. When P-120 fiber is used, the frequency versus pressure scan is similar but the last step cannot be resolved. The difference confirms the claim of the manufacturer that P130-X fiber has more homogeneous surface.[16] The plateau above 0.02 Torr found in the ^{4}He isotherm corresponds to the completion of the second layer; the first layer is expected to be completed well below the resolution of any conventional pressure gauge.[21] Our ^{4}He isotherm up to 1 Torr is qualitatively similar to that taken with exfoliated graphite.[11,20] We did not follow the isotherm to higher pressure since vapor pressure correction, due to the small surface area of the graphite fibers, rapidly becomes the dominant effect.

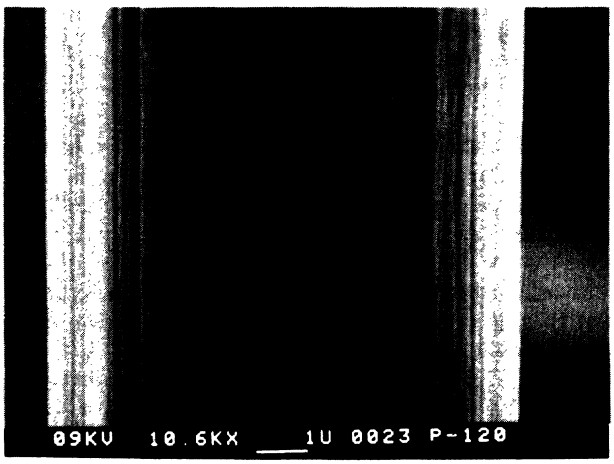

FIG. 1. Scanning electron micrograph of a P-120 graphite fiber. Note the ridge-trough structure of the long and narrow basal-plane facets that run parallel to the fiber axis. The white bar indicates a scale of one micron.

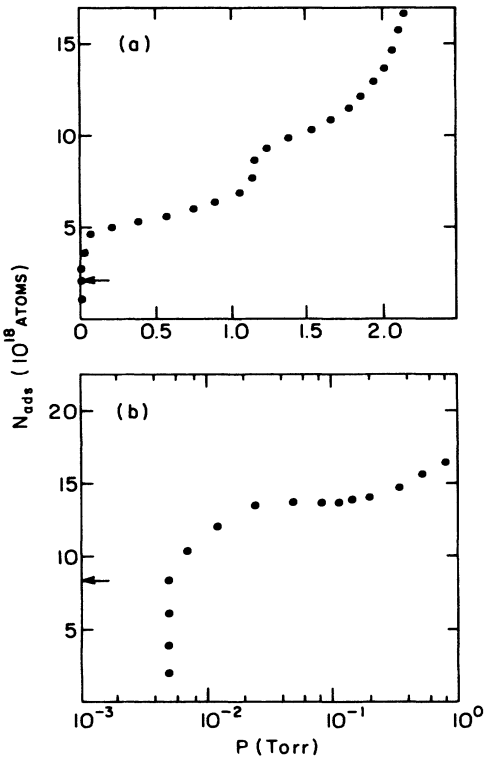

FIG. 2. Adsorption isotherms on graphite fibers of (a) Xe at $T = 113$ K and (b) ^{4}He at $T = 2.16$ K. The arrows indicate the expected amount of adsorption in the first layer for Xe and in the first two layers for ^{4}He, assuming the fibers are perfect cylinders with a diameter of 9.5 μm.

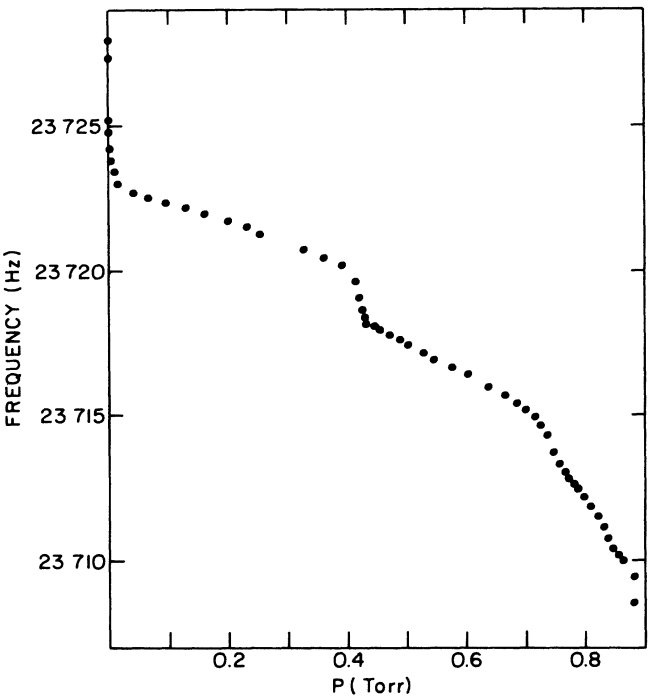

FIG. 3. Resonant frequency of the fiber vs pressure for Xe at $T = 107$ K, note steps at 0.42, 0.73, and 0.84 Torr.

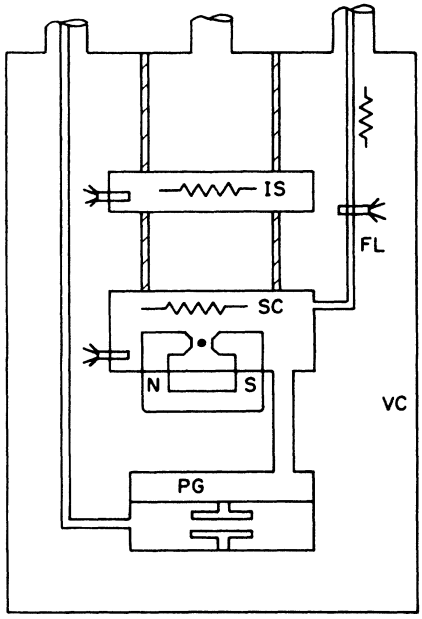

FIG. 4. Schematic drawings of the central part of the cryostat illustrating positions of heaters and thermometers. IS: intermediate stage; FL: fill line; SC: sample cell; NS: permanent magnet; VC: vacuum can; PG: pressure gauge.

If we assume all the fibers are perfectly cylindrical in cross section with an average diameter of 9.5 μm, then the 2.26 gm bundle should have a geometrical surface area of 0.43 m^2. Using the areal density of the first layer of Xe on graphite (0.050 $Å^{-2}$, Refs. 19 and 22) and of the first two layers of ^{4}He on graphite (0.195 $Å^{-2}$, Ref. 20), we expect there should be 2.4×10^{18} atoms of Xe in each layer and 8.4×10^{18} atoms in the first two layers of ^{4}He. According to the Xe and ^{4}He isotherms shown in Fig. 1 the surface area of the bundle accessible for adsorption is, respectively, 2.3 and 1.7 times larger than the simple geometrical value.

III. EXPERIMENTAL APPARATUS

A schematic drawing of the apparatus is shown in Fig. 4. A P-120 graphite fiber, 9 μm in diameter and 1.5 cm long, is mounted under tension to a copper support with silver epoxy. The fiber is situated horizontally inside a copper sample cell approximately 5 cm in diameter and 3 cm high, the fiber is 0.5 cm above the bottom of the cell. A magnetic field of 2.8 kG perpendicular to the fiber axis is provided by two pole pieces, silver soldered through the bottom of the cell and connected to a permanent magnet outside the cell. An *in situ* diaphragm capacitance pressure gauge is connected to the bottom of the sample cell via a 0.64-cm-o.d. copper tubing. The active part of the pressure gauge is an electrode attached to a 0.25 mm thick stainless-steel diaphragm 3 cm in diameter. The capacitance of this movable electrode and a fixed electrode is measured relative to a standard reference capacitor using a standard three-terminal bridge technique. Resolution and stability in the pressure measurement is 1 mTorr, corresponding to a relative resolution of about 1 part in 10^6. Such resolution is important in a wetting experiment since most of the film growth takes place in the last 2% of the pressure range. The fill line to the sample cell is made of a vacuum jacketed thin wall 0.32-cm-i.d., stainless-steel tubing. All electrical leads are thermally anchored to an intermediate stage which acts as a thermal baffle between the sample cell and bath. The sample cell, fill line, and intermediate stage are all equipped with thermometers and electrical heaters. Cooling of the cell is achieved by pumping on a helium bath with weak thermal links from the bath to the intermediate stage and from there to the sample cell. During the experiment, the intermediate stage is typically 0.2 K colder than the cell whereas the fill line is always kept warmer than the cell. This is accomplished by winding a heater around the fill line, controlled by a thermometer anchored on the fill line, 4 cm from the cell. The temperature at the fill line thermometer is kept 1–2 K above that of the sample cell. During the course of an experimental run the temperature of the cell is kept constant to within ±10 μK, as deduced from pressure fluctuations at the saturated vapor pressure.

The fiber is an element in an ac Wheatstone bridge circuit which is balanced outside the resonance region. When the bridge is driven at $f = f_0$, the resonant frequency, an induced voltage 90° out of phase with respect to the excitation voltage, results from the mechanical oscillation of the fiber in the magnetic field. This out-of-phase signal is used to form a phase-locked feedback loop which locks the closed-loop frequency of the voltage-

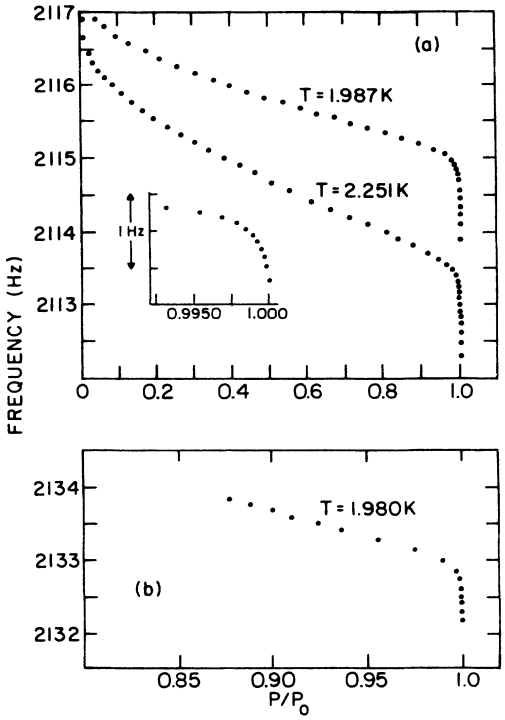

FIG. 5. Resonant frequency of the fiber as a function of pressure for (a) ^{4}He above and below T_λ; (b) ^{3}He at $T=1.980$ K. P_0 is the saturated vapor pressure. The inset shows the data at 2.25 K on an expanded scale close to P_0.

controlled oscillator in the lock-in amplifier to the resonant frequency. The power dissipation due to the drive current is typically less than 40 pW resulting in a temperature rise in the fiber less than a few microkelvin. Small doses of ultra-high-purity helium are added to the cell and the resonant frequency is measured as a function of pressure. Typical results are shown in Fig. 5.

IV. RESULTS AND DISCUSSION

For pressures well below the saturated vapor pressure, P_0, the frequency shift is due almost entirely to the added inertia of the surrounding vapor. The hydrodynamics of a cylinder oscillating in a viscous fluid was first worked out by Stokes.[23] The resonant frequency f of the fiber at some gas density ρ_v due to the viscous drag is

$$f=f_0\left[\frac{\rho_w}{\rho_w+k\rho_v}\right]^{1/2}, \tag{1}$$

where f_0 is the resonant frequency in vacuum, ρ_w the density of the fiber, and k the Stokes k function. This coefficient k is a nonlinear function of the dimensionless parameter q given by

$$q=\frac{r}{2}\left[\frac{2\pi f\rho_v}{\eta}\right]^{1/2}, \tag{2}$$

where r is the radius of the fiber and η the fluid viscosity. The value of k changes most rapidly when q is small causing the frequency to change more rapidly at low gas pressures.

Close to P_0 the frequency drops quickly with increasing pressure due to the added mass of the film. For a film of thickness d and density ρ_l the shift in the resonant frequency due to a film absorbed on the surface of a cylinder is

$$\frac{\Delta f}{f}=-\frac{\rho_l}{\rho_w}\frac{d}{r}. \tag{3}$$

As can be seen from Fig. 5 there is essentially no difference in the wetting behavior above and below the λ point. Several ^{4}He runs were done from 2.0 to 2.8 K and all runs show the same wetting characteristics. Our value of $\Delta f/f$ at P_0 above and below T_λ is in good agreement with the data of TS below T_λ. Only one ^{3}He run was done and is shown in Fig. 5(b). The smaller frequency drop is due to primarily the smaller value of the liquid density. Our pressure resolution is sufficient to indicate that the film is thickening continuously as P_0 is approached. The inset in Fig. 4 shows an example of the frequency shift due to the film close to P_0 on an expanded pressure scale. Quantitatively similar results have been obtained using a P-130X fiber with an operating frequency of 23 kHz, indicating that our results are independent of fiber type and frequency. It is with this fiber that three steps were found in the Xe isotherm shown in Fig. 3.

When an adsorbate completely wets a substrate, the film thickness is usually compared with the Frenkel-Halsey-Hill (FHH) relation[24]

$$d=\left[\frac{k_BT}{\alpha(d)}\ln\frac{P_0}{P}\right]^{-1/3}, \tag{4}$$

where $\alpha(d)$ characterizes the strength of the absorbate-substrate interaction and the $-\frac{1}{3}$ exponent reflects the nature of the van der Waals attraction. The FHH relation can be considered as an approximation of the DLP theory in the region where the film is of intermediate thickness, it is of sufficient thickness (more than two or three layers) that continuum approximation of the substrate is valid and not so thick that retardation effect becomes important.[25] In our experimental configuration, two corrections are expected:[12]

$$d=\left[\frac{k_BT}{\alpha(d)}\right]^{-1/3}\left[\ln\frac{P_0}{P}+\frac{\sigma v}{rk_BT}+\frac{mgh}{k_BT}\right]^{-1/3}, \tag{5}$$

where m is the mass of a helium atom, σ the liquid-vapor surface tension, v the volume per atom, r the radius of the fiber, and $h=0.5$ cm is the height of the fiber from the bottom of the sample cell. The value of the surface tension term is 2.0×10^{-4} K and the gravity term is 2.4×10^{-5} K. Therefore, these two correction terms become significant when the pressure is within 0.1% and 0.01%, respectively, of the saturated vapor pressure. We have used the distance from the fiber to the bottom of the sample cell instead of the distance to the pressure gauge because we observed no difference in film thickness before

and after the pressure gauge was installed. This is reasonable because the pressure gauge is probably at a slightly higher temperature than that of the sample cell. The gauge, as shown in Fig. 4, is cooled through the sample cell. In any case, and as discussed above, the gravity term is negligible except for pressure very close to P_0; even then the film thickness may be dominated by the possible surface tension term.

Because of the additional surface area, Eq. (3) is not strictly applicable to graphite fibers used in our experiment. In the data analysis on the microbalance results we have found that a correction factor to the geometric surface area of 2.7 gives the best agreement between theory and experiment. A value of (43 K)k_B(layers)^3 (Ref. 26) is used for $\alpha(d)$ in Eqs. (4) and (5). For helium and our experiment setup, this corresponds to a frequency shift of 0.03 Hz per layer. This correction factor is higher than the factor of 2 determined from the volumetric adsorption isotherms. We can think of at least two possible explanations for the discrepancy. Firstly, our assumption of uniform diameter and specific surface area for each fiber used in arriving at the simple geometrical surface area is unlikely to be exact. Electron microscope pictures taken by us and other workers[13,27] on several fibers found a variation of diameter of at least 10%. Secondly, the fiber used in the microbalance measurement was heated *in situ* to at least 600 K inside a copper cell that was maintained at 4.2 K. Such a cleaning procedure was not possible for the bundle of fibers used in the volumetric vapor pressure isotherm study. Based on our experience with exfoliated graphite substrates, less rigorous cleaning of the substrate often results in smaller specific surface area.

An analysis of the $T=2.251$ K isotherm is shown in Fig. 6. A "background" isotherm done at $T=2.45$ K, consisting almost entirely of the hydrodynamic frequency shift is subtracted off the 2.251 K isotherm leaving Δf, that part of the frequency shift due to the film. We have found experimentally that for small changes in temperature the hydrodynamic contribution can be regarded as essentially pressure dependent. This procedure slightly underestimates the true frequency shift because Eq. (4) predicts that the background taken at 2.45 K also contains approximately three layers when the pressure is at the value corresponding to P_0 at 2.251 K. This three layers correction is subtracted from the 2.45 K isotherm to be the true hydrodynamically corrected background for the 2.251 K isotherm. It is evident from Fig. 6 that our data are in good agreement with the theoretical prediction, including the expected $-\frac{1}{3}$ exponent. It should be noted that data shown in Fig. 5 ranges from $P/P_0=0.88$ to 0.9999 or three decades in $\ln(P/P_0)$. To our knowledge the only other quantitative study of the wetting properties of ^{4}He on graphite compares their data from $P/P_0=0.75$ to approximately 0.99, or slightly more than one decade in $\ln(P_0/P)$ (Ref. 9). The reduced pressure range in Fig. 6 is comparable to the experiment of Sabisky and Anderson.[7]

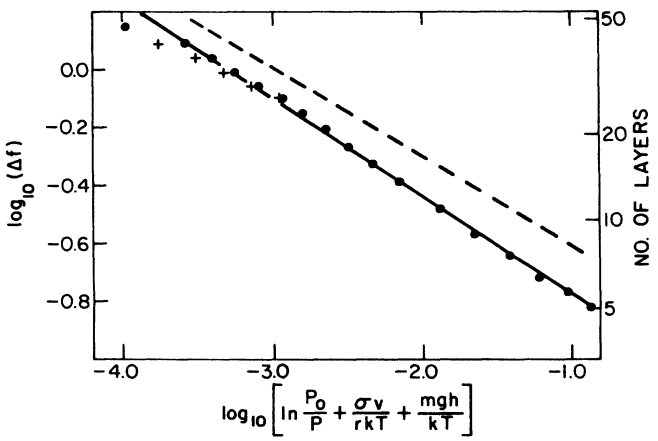

FIG. 6. Analysis of the $T=2.251$ K isotherm according to Eq. (5). The scale on the right indicates the number of layers using a value for the sensitivity of 0.03 Hz/layer. The solid line is the theoretical curve calculated from Eq. (5) showing an exponent of $-\frac{1}{3}$. Data are plotted accounting for (solid dots) and neglecting (crosses) the effect of surface tension. For comparison the dashed line is drawn with an exponent of -0.3.

Because the surface is partly comprised of flat facets with dimensions larger than the film thickness, it is possible that the correction term in Eq. (5) overestimates the surface tension effect. In Fig. 6 the data are also analyzed without the surface tension term. The sign and magnitude of the deviation of the data from the $-\frac{1}{3}$ straight line as P approaches P_0 is consistent with the retardation effect expected of very thick films.[25] However, a quantitative comparison of the ^{3}He and ^{4}He data in Fig. 5 appears to support the existence of the surface tension effect. Using Eq. (5) we have calculated the theoretical change in film thickness from $P/P_0=0.99$ to 1.00 for both ^{3}He and ^{4}He with and without the surface tension term. Values for the surface tension of ^{3}He and ^{4}He were taken from Ref. 28. From Eq. (3) we then calculate the ratio of the expected frequency shift for ^{3}He to that of ^{4}He over the same reduced pressure range. When the surface tension term is included this theoretical ratio is 0.74, experimentally we measure a value of 0.77. If the surface tension term is omitted, the value of the ratio becomes 0.59. Therefore, although the fiber is not a perfect cylinder of radius r, our experimental results clearly suggest that we treat the surface as having an average radius of curvature close to the macroscopically measured value. When the surface tension term is included in the analysis, it is evident from Fig. 6 that we do not observe the effect of retardation. It is possible that size effects, which tend to produce a thicker film than what is predicted from Eq. (5) [Ref. 29], are nearly canceling out the effect of retardation.

An important point to consider is whether or not the ridge-trough structure of the basal plane facets affects the wetting nature of the film. We have evidence clearly indicating that it does not. Using this same microbalance technique, we have done isotherms of N_2 above and below the triple point T_t. Below T_t, the frequency versus pressure scan indicates the formation of a film of N_2 only a few layers thick. As T_t is approached from below, a

continuous increase of the maximum film thickness is found. Above T_t, complete wetting is found. This is consistent with triple-point wetting of a wide number of physisorbed systems observed by a number of other techniques.[3,14,30] The growth mode of Ar on graphite is recently studied by Bruschi, Torzo, and Chan[27] also using a vibrating microbalance technique with P-100 and P-120 fibers. Instead of passing ac current through the fiber the fiber is set in resonance by mechanical means. Triple-point wetting and excellent agreement with the FHH equation is found over two and a half decades in reduced temperature $[8\times10^{-5}<t=(T_t-T)/T_t<10^{-2}]$ and between $P/P_0=0.92$ and $P/P_0=0.999\,68$, slightly less than three decades in $\ln(P_0/P)$. These authors reported their data in terms of mass loading rather than film thickness. Their data are also consistent with the interpretation that the available surface area for adsorption is much more than that of the geometrical value. These results on the triple-point wetting systems and the apparent nonwetting result of ^{4}He in the presence of a temperature gradient, discussed below, lead us to conclude that the ridgelike surface structure contributes only extra surface area but does not alter the wetting behavior of the adsorbed film. Electron micrograph pictures on the cross section of a broken fiber indicate the amplitude of the ridge-trough surface structures is also on the order of 0.1 μm, similar to that of the width. Since the maximum film thickness in our experiment is only on the order of 100 Å, we do not expect capillary condensation on the surface to be of importance for most of the thickness range of our experiment (see thickness scale in Fig. 6). The fact that we do not see any upward deviation from the expected and observed-$\frac{1}{3}$ power law in Fig. 6 is consistent with this interpretation.

Because of the similarities between our experiment and that of TS, we think the most reasonable explanation of the conflicting results is that the apparent nonwetting they observe is a result of temperature inhomogeneities in their sample cell which may be a result of their particular method of temperature regulation. We were able to simulate incomplete wetting above T_λ in the following manner. By adding a small amount of ^{4}He exchange gas into the vacuum can (VC), the entire low-temperature apparatus reaches a temperature close to that of the bath. Then, with enough gas in the sample cell to be at P_0 over the desired temperature range, the exchange gas in the VC is pumped out and the cell is controlled 0.2 K warmer than the bath. In contrast to the experimental configuration described above, a strong thermal link (thick copper foil) is now installed connecting the bath and the fill-line capillary at the location of the fill-line thermometer. This thermal link ensures that the thermometer region of the capillary is now at a lower temperature than the cell and close to the lowest temperature in contact with the helium gas. What we found is that helium gas condenses out at this spot leaving the cell undersaturated, giving rise to an apparent incomplete wetting observation on the fiber. While maintaining the temperature of the sample cell, the bath is then allowed to warm up slowly causing the fill line also to warm up. As the temperature of the fill line approaches that of the cell,

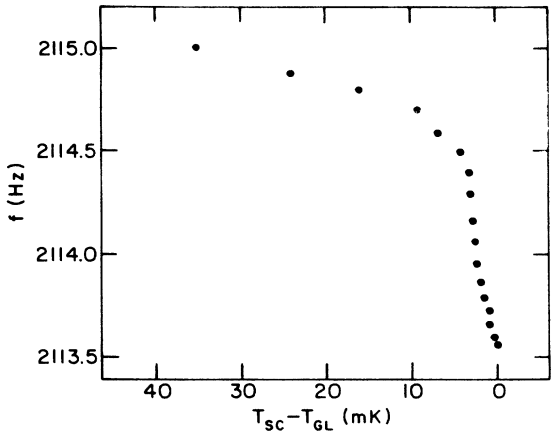

FIG. 7. Resonant frequency of the fiber as a function of the temperature difference between the sample cell and the fill line above T_λ.

helium gas in the cell approaches saturation and the frequency of the fiber drops. Figure 7 shows the resonant frequency as a function of the temperature difference between the sample cell and the cold point on the capillary. The relative temperature scale is established by cross calibrating the fill line and sample cell thermometer with the VC saturated with helium gas. The transition from a film only a few layers thick to a completely wet thick film takes place over a temperature range of about 5 mK. We attempted to repeat the same procedure below T_λ but found it difficult to keep the fill line colder than the sample cell for a time long enough to take data, presumably because of the large thermal conductivity of the film.

The above result does not explain the ^{3}He result of TS, where their sample cell is immersed in superfluid. One possibility is that the incomplete wetting is actually a metastable state resulting from temperature fluctuations. By making a small temperature change after the completion of an isotherm, we also found that the resonant frequency changes to a value that indicates incomplete wetting. The recovery to the expected wetting value often requires more than 2 h. This indicates that true equilibrium conditions are extremely important at and close to P_0.

Since we have characterized the graphite fiber substrate in substantial detail, and we have studied a number of different systems, we are able to give reasonable explanations of a number of anomalous results reported in other papers. In the original experiment using the graphite fiber microbalance, Bartosch and Gregory reported an adsorption exponent for O_2 films below the triple point significantly different from the expected $-\frac{1}{3}$ value. These authors have failed to take into account both the "extra" surface area and the hydrodynamic background. Below T_t where there exists a film only a few layers thick, the frequency shift is dominated by the hydrodynamic drag. Failure to account for this effect would certainly lead to an erroneous value for the adsorption exponent. In contrast, Bruschi, Torzo, and Chan,[27] as stated previously,

do see the expected $-\frac{1}{3}$ exponent in their vibrating fiber experiment of Ar on graphite, when the hydrodynamic effect is substracted. It is also worth pointing out that Bartosch and Gregory have apparently mistaken the initial hydrodynamic frequency drop to be evidence of the first layer. In another experiment, Taborek has studied several classical liquids above their respective triple points.[31] Whereas the hydrodynamic and surface tension effects were properly accounted for in the experiment, the "extra" surface area apparently was not. In the latter paper, P-120 fibers, same as those used here, and fibers grown by pyrolysis of a hydrocarbon vapor were used by Taborek. In contrast, Thornel-type fiber, also manufactured by Amoco but of lower quality than P-120 were used by Bartosch and Gregory.

In summary, using the graphite fiber microbalance technique we have found complete wetting of helium on graphite above and below the λ point. Moreover, we have demonstrated experimentally that incomplete wetting found previously is probably a thermal artifact. A more careful characterization of the graphite fiber surface has revealed that the actual surface area of the fiber is at least twice the geometric surface area. When the additional surface area is taken into account, we find excellent agreement between our data and that predicted from the Frenkel-Halsey-Hill model of adsorption.

ACKNOWLEDGMENTS

We wish to acknowledge useful discussions with L. Bruschi, D. Finotello, K. Gillis, J. Reppy, G. Torzo, and especially E. Cheng, M. Cole, and P. Taborek. We are particularly grateful to R. Bacon, who provided us with the fibers and patiently answered our questions. This work is supported by the National Science Foundation (NSF) through Grant Nos. DMR-84-19261 and DMR-87-18771. One of us (M.H.W.C.) also acknowledges support from the Guggenheim Foundation.

[1]R. Pandit, M. Schick, and M. Wortis, Phys. Rev. B **26**, 5112 (1982); D. E. Sullivan, *ibid.* **20**, 3991 (1979).

[2]S. Rauber, J. R. Klein, M. W. Cole, and L. W. Bruch, Surf. Sci. **123**, 173 (1982).

[3]J. L. Seguin, J. Suzanne, M. Bienfait, J. G. Dash, and J. A. Venables, Phys. Rev. Lett. **51**, 122 (1983).

[4]F. Gittes and M. Schick, Phys. Rev. B **30**, 209 (1984); D. A. Huse, *ibid.* **29**, 6985 (1984).

[5]A. C. Ham and L. C. Jackson, Proc. R. Soc. London, Ser. A **240**, 243 (1959); L. G. Grimes and L. C. Jackson, Philos. Mag. **4**, 1346 (1959).

[6]D. Hemming, Can. J. Phys. **49**, 2621 (1971).

[7]E. S. Sabisky and C. H. Anderson, Phys. Rev. A **7**, 790 (1973).

[8]I. E. Dzyaloshinskii, E. M. Lifshitz, and L. P. Pitaevskii, Adv. Phys. **10**, 165 (1961).

[9]A. D. Migone, J. Krim, J. G. Dash, and J. Suzanne, Phys. Rev. B **31**, 7643 (1985).

[10]M. J. Lea, D. S. Spencer, and P. Fozooni, Phys. Rev. B **35**, 6665 (1987).

[11]M. Bienfait, J. G. Dash, and J. Stoltenberg, Phys. Rev. B **21**, 2765 (1980).

[12]S. Kumar, T. Brosius, G. Torzo, D. Finotello, and J. D. Maynard, Phys. Rev. B **37**, 7352 (1988).

[13]P. Taborek and L. Senator, Phys. Rev. Lett. **57**, 218 (1986).

[14]J. T. Tough, W. D. McCormick, and J. G. Dash, Phys. Rev. **132**, 2373 (1973).

[15]C. Bartosch and S. Gregory, Phys. Rev. Lett. **54**, 2513 (1985).

[16]Fibers provided by R. Bacon of Amoco Performance Products, Inc., Parma Technical Center, 12900 Snow Road, Parma, Ohio 44130.

[17]R. Bacon, *Mesophase Pitch-Based and Other Carbon Fibers,* Paper presented at Workshop on Transverse Tensile Strength in Carbon-Fiber/Aluminum Composite, 1984, edited by R. in Carbon-Fiber/Aluminum Composite, 1984, edited by R. N. Lee (unpublished).

[18]C. B. Ng, G. W. Henderson, M. Buechlev, and J. L. White, *American Carbon Society, 16th Biennial Conference in Carbon, Extended Abstracts, July 1983* (University of California, San Diego; San Diego, California), p. 515.

[19]A. Thomy and X. Duval, J. Chim. Phys. **67**, 286 (1970).

[20]S. E. Polanco and M. Bretz, Surf. Sci. **94**, 1 (1980).

[21]R. L. Elgin and D. L. Goodstein, Phys. Rev. A **9**, 2657 (1974).

[22]N. J. Colella and R. M. Suter, Phys. Rev. B **34**, 2052 (1986).

[23]G. G. Stokes, *Mathematical and Physical Papers* (Cambridge University Press, London, 1922), Vol. 3, p. 38.

[24]J. Frenkel, *Kinetic Theory of Liquids* (Oxford, New York, 1949); G. D. Halsey, Jr., J. Chem. Phys. **16**, 931 (1948); T. L. Hill, *ibid.* **17**, 590 (1949).

[25]E. Cheng and M. W. Cole, Phys. Rev. B **38**, 987 (1988).

[26]G. Vidali, M. W. Cole, and C. Schwartz, Surf. Sci. **87**, L273 (1979).

[27]L. Bruschi, G. Torzo, and M. H. W. Chan, Europhys. Lett. **6**, 541 (1988).

[28]D. O. Edwards and W. F. Saam, *Progress in Low Temperature Physics* VIIa, edited by D. F. Brewer (North-Holland, Amsterdam, 1978), pp. 283–369.

[29]N. K. Mahale and M. W. Cole, Surf. Sci. **172**, 311 (1986).

[30]See for example, Q. M. Zhang, Y. P. Feng, H. K. Kim, and M. H. W. Chan, Phys. Rev. Lett. **57**, 1456 (1987); A. D. Migone, J. G. Dash, M. Schick and O. E. Vilches, Phys. Rev. B **34**, 6322 (1986); S. G. J. Mochrie, M. Sutton, R. J. Birgeneau, D. E. Moncton, and P. M. Horn, *ibid.* **30**, 263 (1984); J. Krim, J. P. Coulomb, and J. Bonzidi, Phys. Rev. Lett. **58**, 583 (1987); M. Drir and G. B. Hess, Phys. Rev. B **33**, 4758 (1986); R. Pandit and M. E. Fisher, Phys. Rev. Lett. **51**, 1772 (1983).

[31]P. Taborek (unpublished).

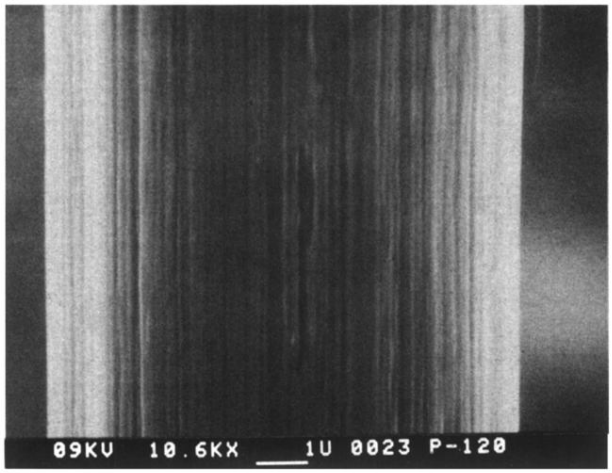

FIG. 1. Scanning electron micrograph of a P-120 graphite fiber. Note the ridge-trough structure of the long and narrow basal-plane facets that run parallel to the fiber axis. The white bar indicates a scale of one micron.